The Effect of Electron-Phonon Interaction on the Static and Dynamic Response of CNTFETs

M. Pourfath*, H. Kosina*, B.H. Cheong†, W.J. Park‡, and S. Selberherr*

* Institute for Microelectronics, TU Wien, Gußhausstraße 27–29/E360, 1040 Wien, Austria
Phone: +43-1-58801/36031, Fax: +43-1-58801/36099, E-mail: pourfath@iue.tuwien.ac.at

† Computational Science and Engineering Lab,‡ Materials and Devices Lab
Samsung Advanced Institute of Technology, Suwon 440-600, Korea.

***Abstract*— The non-equilibrium Green's function formalism is employed to perform a comprehensive numerical study of carbon nanotube field-effect transistors. Due to numerous possible configurations of CNTs many different material parameters exists. The static and dynamic response of transistors is studied for a wide range of electron-phonon interaction parameters.**

I. Introduction

A carbon nanotube (CNT) can be viewed as a rolled-up sheet of graphite with a diameter of a few nano-meters. Depending on the chiral angle the CNT can be either metallic or semiconducting. Semiconducting CNTs can be used as channels for field-effect transistors (FETs). CNTFETs have been studied in recent years as potential alternatives to CMOS devices because of their capability of near ballistic transport.

Depending on the work function difference between the metal contact and the CNT, carriers at the metal-CNT interface encounter different barrier heights. Devices with positive [1, 2] and zero [3] barrier heights were fabricated. The barrier height is defined as the potential barrier which is seen by carriers at the metal Fermi level. Therefore, in a device with zero barrier height, carriers with energies above the metal Fermi level reach the channel by thermionic emission and those below the Fermi level have to tunnel to reach the channel. Devices with positive barrier height have lower on-current and also suffer from ambipolar behavior [4–8], while devices with zero barrier height theoretically [9] and experimentally [10] show better performance. In this work we focus on devices with zero barrier height for electrons. Since the dispersion relations for electrons and holes are the same, our discussions are valid for holes as well [11].

The non-equilibrium Green's function (NEGF) formalism has been successfully used to investigate the characteristics of nano-meter silicon transistors [12, 13], carbon nanotube based transistors [9, 14–16], and molecular devices [17]. In this work the NEGF formalism is used to investigate the effect of electron-phonon interaction on the static and dynamic response of CNTFETs.

II. Approach

In this section the models used to study the static and dynamic response of CNTFETs are described.

A. Static Response

Due to quantum confinement along the tube circumference, carriers have bound wave functions around the CNT and can propagate along the tube axis. Under the assumption that the potential profile does not vary around the circumference of the CNT, sub-bands will be decoupled [12]. In this work we assume bias conditions for which the first sub-band contributes mostly to the total current. In the mode-space approach the transport equation for each sub-band can be written as [18]:

$$G^{\mathrm{R,A}}_{\mathbf{r},\mathbf{r}'}(E) = [EI - H_{\mathbf{r},\mathbf{r}'}(E) - \Sigma^{\mathrm{R,A}}_{\mathbf{r},\mathbf{r}'}(E)]^{-1} \tag{1}$$

$$G^{<,>}_{\mathbf{r},\mathbf{r}'}(E) = G^{\mathrm{R}}_{\mathbf{r},\mathbf{r}'}(E)\Sigma^{<,>}_{\mathbf{r},\mathbf{r}'}(E)G^{\mathrm{A}}_{\mathbf{r},\mathbf{r}'}(E) \tag{2}$$

In (1) an effective mass Hamiltonian was assumed. A recursive Green's function method is used for solving (1) and (2) [13]. The total self-energy in (1) consists of the self-energies due to the source contact, drain contact, and electron-phonon interaction, $\Sigma^R = \Sigma^R_{\mathrm{S}} + \Sigma^R_{\mathrm{D}} + \Sigma^R_{\mathrm{el-ph}}$. The self-energy due to electron-phonon interaction comprises contributions of elastic and inelastic scattering mechanisms, $\Sigma^{<,>}_{\mathrm{e-ph}} = \Sigma^{<,>}_{\mathrm{el}} + \Sigma^{<,>}_{\mathrm{inel}}$. Assuming a single sub-band the electron-phonon self-energies are simplified to the set (3) to (6).

$$\Sigma^{<,>}_{\mathrm{el},(\mathbf{r},\mathbf{r})}(E) = D_{\mathrm{el}}G^{<,>}_{\mathbf{r},\mathbf{r}}(E) \tag{3}$$

$$\begin{aligned}\Sigma^{<}_{\mathrm{inel},(\mathbf{r},\mathbf{r})}(E) = \sum_{\nu} D^{\nu}_{\mathrm{inel}} \\ \times[(n_B(\hbar\omega_\nu)+1)G^{<}_{\mathbf{r},\mathbf{r}}(E+\hbar\omega_\nu) \\ +n_B(\hbar\omega_\nu)G^{<}_{\mathbf{r},\mathbf{r}}(E-\hbar\omega_\nu)]\end{aligned} \tag{4}$$

$$\begin{aligned}\Sigma^{>}_{\mathrm{inel},(\mathbf{r},\mathbf{r})}(E) = \sum_{\nu} D^{\nu}_{\mathrm{inel}} \\ \times[(n_B(\hbar\omega_\nu)+1)G^{>}_{\mathbf{r},\mathbf{r}}(E-\hbar\omega_\nu) \\ +n_B(\hbar\omega_\nu)G^{>}_{\mathbf{r},\mathbf{r}}(E+\hbar\omega_\nu)]\end{aligned} \tag{5}$$

$$\Im m[\Sigma^{\mathrm{R}}(E)] = \frac{1}{2i}[\Sigma^{>} - \Sigma^{<}] \tag{6}$$

$$\Re e[\Sigma^{\mathrm{R}}_{\mathrm{e-ph}}(E)] = \frac{1}{\pi}\mathbf{P}\int \frac{\Im m[\Sigma^{\mathrm{R}}_{\mathrm{e-ph}}(E')]}{E'-E}dE' \tag{7}$$

where n_B is given by the Bose-Einstein distribution function. In general electron-phonon interaction parameters ($D_{\mathrm{el,inel}}$) depends on the diameter and the chirality of the CNT [19].

 1-4244-0404-5/06/$20.00

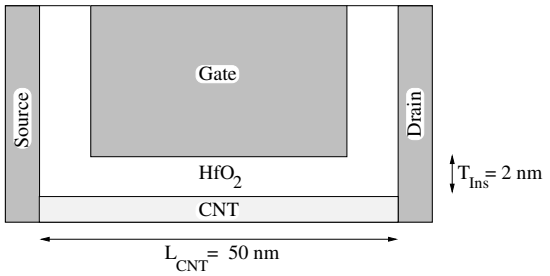

Figure 1: Cross section of the device.

The self-energy is added to the Hamiltonian. The imaginary part of the self-energy (6) broadens the density of states, whereas the real part of the self-energy (7) shifts the density of states. Even for strong electron-phonon coupling the real part is about several 10 meV (Fig. 2), which is often negligible compared to the electrostatic potential.

The transport equations are iterated to achieve convergence of the electron-phonon self-energies, resulting in a self-consistent Born approximation.

The carrier concentration and the current density at some position $\mathbf{r}$ of the device can be calculated as (8) and (9).

$$n_{\mathbf{r}} = -4i \int G^{<}_{\mathbf{r},\mathbf{r}}(E) \frac{dE}{2\pi} \tag{8}$$

$$j_{\mathbf{r}} = \frac{4q}{\hbar} \int \mathrm{Tr}[\Sigma^{<}_{\mathbf{r},\mathbf{r}} G^{>}_{\mathbf{r},\mathbf{r}}(E) - \Sigma^{>}_{\mathbf{r},\mathbf{r}} G^{<}_{\mathbf{r},\mathbf{r}}(E)] \frac{dE}{2\pi} \tag{9}$$

In the Poisson equation carriers are treated as a sheet charge distributed over the surface of the CNT. After convergence of the scattering self energies, the coupled system of transport and Poisson equations is solved iteratively. Details are presented in [20].

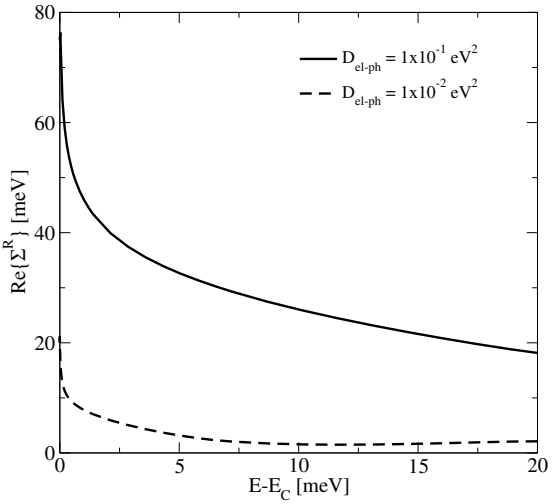

Figure 2: The real part of $\Sigma^{R}_{\mathrm{e-ph}}$ versus energy for elastic scattering with the band-edge of the conduction band as the reference. Even for strong electron-phonon coupling this term is about several 10 meV, which is negligible compared to the electrostatic potential.

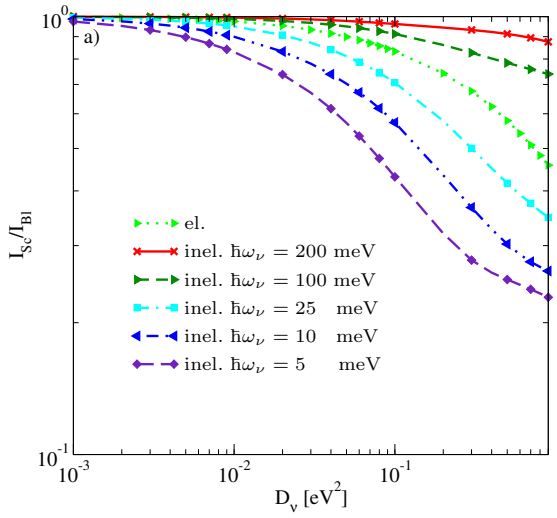

Figure 3: The ballisticity versus the strength of electron-phonon coupling for a CNT of 50 nm length.

B. Dynamic Response

To investigate the dynamic response of the device we consider the device delay time defined as:

$$\tau = \frac{C_{\mathrm{G}} V_{\mathrm{DD}}}{I_{\mathrm{on}}} \tag{10}$$

Here, ${C_{\mathrm{G}}}^{-1} = {C_{\mathrm{Ins}}}^{-1} + {C_{\mathrm{Q}}}^{-1}$. The quantum capacitance is given by $C_{\mathrm{Q}} = 8\mathrm{q}^2/\mathrm{h}\nu_{\mathrm{F}} \approx 400\mathrm{aF}/\mu\mathrm{m}$, including the twofold band and spin degeneracy [21]. We assume the quantum capacitance limit, where $C_{\mathrm{Q}} \ll C_{\mathrm{Ins}}$.

The device delay time versus the $I_{\mathrm{on}}/I_{\mathrm{off}}$ ratio can be used to compare devices with different geometries and material properties [22].

III. Simulation Results

All our calculations assume a CNT with a band gap of $\mathrm{E_g} = 0.6$ eV corresponding to a diameter of $\mathrm{d_{CNT}} = 1.6$ nm, and $m^* = 0.05 m_0$ for both electrons and holes. Due to numerous possible configurations of CNTs many different material parameters exists. In the following the device response is studied for a wide range of electron-phonon interaction parameters.

To compare the effect of different scattering mechanisms, we define the ballisticity as the ratio of the current in the presence of electron-phonon interaction to the current in the ballistic case ($I_{\mathrm{Sc}}/I_{\mathrm{Bl}}$). With increasing D_ν the self-energy increases, (3) to (7), which adds dissipation to the Hamiltonian, and consequently the total current decreases. Fig. 3 shows the ballisticity as a function of D_ν. Elastic scattering conserves the energy of carriers, but the current decreases due to elastic back-scattering. On the other hand, with inelastic scattering the energy of carriers is not conserved. Carriers acquiring enough kinetic energy can emit phonons and scatter into lower energy states. With the increase of $\hbar\omega_\nu$ the current is less reduced, since scattered carriers lose more kinetic energy and

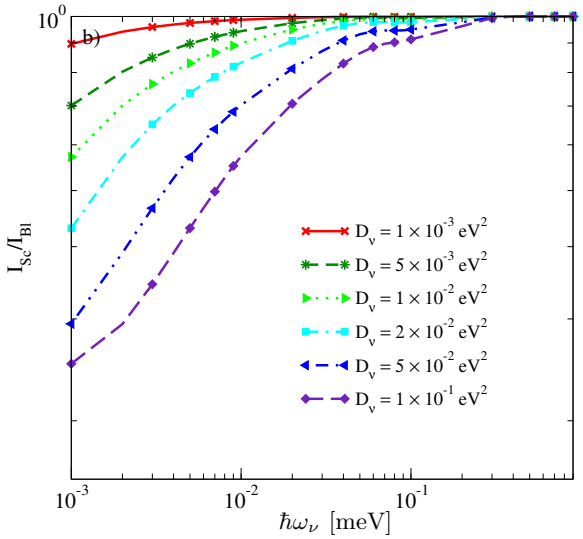

Figure 4: The ballisticity versus the phonon energy for a CNT of 50 nm length.

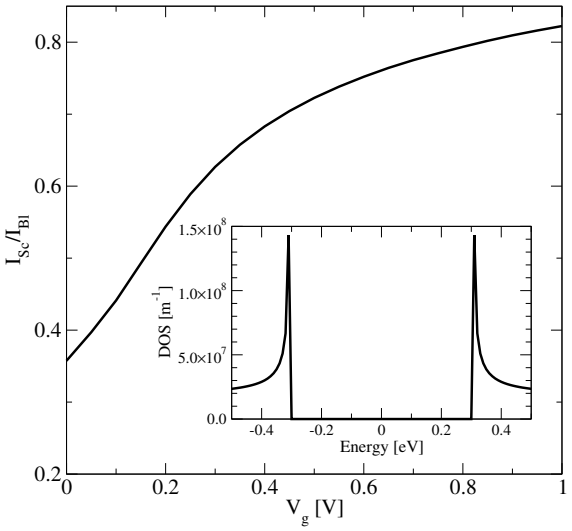

Figure 6: The ballisticity as a function of gate voltage in the presence of elastic scattering ($D_{\rm el} = 10^{-1}$ eV^2). The inset shows one-dimensional density of states for the first sub-band.

the probability for back-scattering decreases [23], see Fig. 4. These results are for a CNT of 50 nm length. Fig. 5 shows that the ballisticity is inversely proportional to the CNT length.

Next we investigate the role of the gate voltage on the ballisticity. Fig. 6 shows the ballisticity in the presence of elastic scattering as a function of the gate voltage. With increasing gate voltage the ballisticity decreases. The inset of Fig. 6 shows the density of states due to the first sub-band of the described CNT. At low gate voltages the Van Hove singularity of the one-dimensional density of states is close to metal Fermi level. Therefore, for the majority of injected carriers the scattering rate is high and the ballisticity decreases.

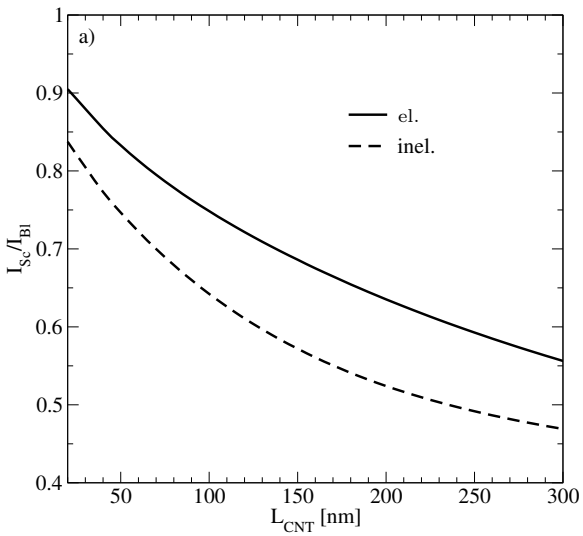

Figure 5: Ballisticity versus CNT length. The following parameters were used for elastic scattering $D_{\rm el} = 10^{-1}$ eV^2 and for inelastic scattering $D_{\rm inel} = 10^{-1}$ eV^2 and $\hbar\omega_{\rm inel} = 25$ meV.

As the gate voltage increases the Van Hove singularity is pushed far below the Fermi level, and as a consequence the ballisticity increases. It should be mentioned that this behavior continues until the next sub-band crosses the Fermi level.

Fig. 7 compares the device delay time versus the $I_{\rm on}/I_{\rm off}$ ratio with and without scattering. Similar to the static response, with increasing electron-phonon coupling the device delay time increases considerably. In case of inelastic scattering with high energy phonons the device performance is weakly affected.

IV. Discussion

Elastic scattering occurs due to acoustic phonons and inelastic scattering due to zone boundary (ZB), optical (OP), and radial breathing (RBM) phonon modes. The energies of the these phonon modes are $\hbar\omega_{\rm ZB} \approx 160$ and 180 meV, $\hbar\omega_{\rm OP} \approx 200$ meV, and $\hbar\omega_{\rm RBM} \approx 30$ meV [24]. The corresponding electron-phonon interaction coupling strength depends on the chirality and the diameter of the CNT. The theoretical estimation of these parameters is presented in [19]. As a rough estimate for nanotubes with a diameter of $d_{\rm CNT} = 1-2$ nm the corresponding coupling coefficients are $D_{\rm ZB,OP} < 50\times10^{-3}$ eV^2 and $D_{\rm RBM} < 10^{-3}$ eV^2 [24, 25]. As discussed in the previous section for devices shorter than several hundred nano-meters, high energy phonons, such as OP and ZB phonon modes, degrade the performance only weakly, whereas the RBM phonon mode can have a detrimental effect. However, due to weak electron-phonon coupling, the RBM mode has a negligible effect at room temperature. The electron-phonon coupling is also weak for acoustic phonon (AP) modes ($D_{\rm AP} \approx 10^{-4}$ eV^2), which implies weak elastic backscattering of carriers. Therefore, short CNTFETs can operate close to the ballistic limit [10].

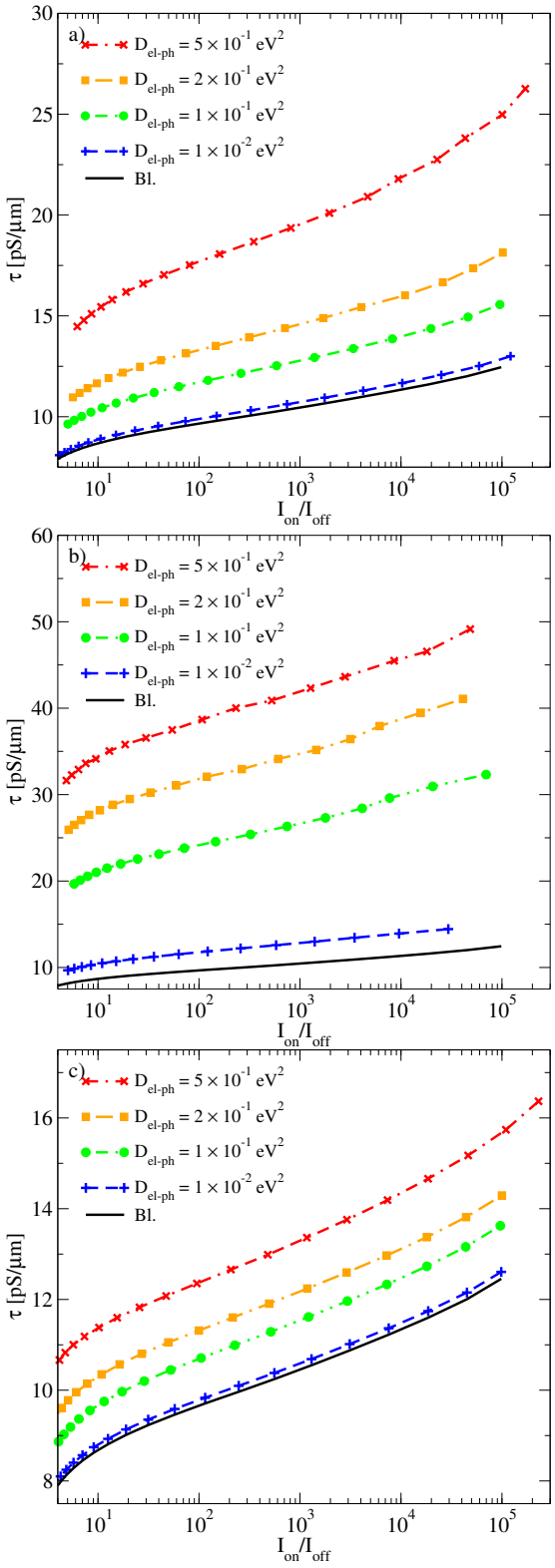

Figure 7: The effect of electron-phonon interaction on the device delay time versus the $I_{\rm on}/I_{\rm off}$ ratio for (a) elastic scattering, (b) inelastic scattering with $\hbar\omega_\nu = 5$ meV, and (c) inelastic scattering with $\hbar\omega_\nu = 100$ meV

V. Conclusion

Based on the NEGF formalism we investigated the effect of electron-phonon interaction on the performance of CNTFETs. For elastic scattering, the electron-phonon coupling strength plays an important role. For inelastic scattering not only the coupling strength, but also the phonon energy is an important factor. In CNTs either the electron-phonon coupling is weak or the phonon energies are high. Therefore, the performance of short devices is only weakly affected.

Acknowledgment

This work has been partly supported by the Austrian Science Fund, contract I79-N16, and the national program for tera-level nano-devices of the Korean ministry of science and technology.

References

[1] J. Appenzeller *et al.*, Phys.Rev.Lett. **92**, 048301 (2004).
[2] M. Radosavljevic *et al.*, Appl.Phys.Lett. **83**, 2435 (2003).
[3] A. Javey *et al.*, Letters to Nature **424**, 654 (2003).
[4] R. Martel *et al.*, Phys.Rev.Lett. **87**, 256805 (2001).
[5] M. Freitag *et al.*, **93**, 076803 (2004).
[6] M. Pourfath *et al.*, in *Proc. ESSDERC* 429 (2004)
[7] M. Pourfath *et al.*, J.Appl.Phys. **97**, 1061031 (2005).
[8] M. Pourfath *et al.*, Microelectronic Engineering **81**, 428 (2005).
[9] J. Guo *et al.*, IEEE Trans. Electron Devices **51**, 172 (2004).
[10] A. Javey *et al.*, Nano Lett. **4**, 1319 (2004).
[11] R. Saito *et al.*, *Physical Properties of Carbon Nanotubes* (Imperial College Press, 1998).
[12] R. Venugopal *et al.*, J.Appl.Phys. **92**, 3730 (2002).
[13] A. Svizhenko *et al.*, J.Appl.Phys. **91**, 2343 (2002).
[14] A. Svizhenko *et al.*, Phys.Rev.B **72**, 085430 (2005).
[15] J. Guo, J.Appl.Phys. **98**, 063519 (2005).
[16] A. Svizhenko *et al.*, IEEE Trans.Nanotechnology **4**, 557 (2005).
[17] W. Tian *et al.*, J.Chem.Phys **109**, 2874 (1998).
[18] S. Datta, *Electronic Transport in Mesoscopic Systems* (Cambridge University Press, 1995).
[19] G. Mahan, Phys.Rev.B **68**, 125409 (2003).
[20] M. Pourfath *et al.*, Lecture Notes in Computer Science **3743**, 578 (2006).
[21] D. John *et al.*, J.Appl.Phys. **96**, 5180 (2004).
[22] J. Guo *et al.*, in *IEDM Tech.Dig.* 703 (2004)
[23] J. Guo *et al.*, Appl.Phys.Lett. **86**, 193103 (2005).
[24] J. Park *et al.*, Nano Lett. **4**, 517 (2004).
[25] S. Koswatta *et al.*, cond-mat/0511723 (2005).